

Isothermal Diffusion and Trapping of Helium in a Silver-Lithium-Alloy after Neutron Irradiation

H. Gaus, H. Migge, and K.-D. Mirus

Hahn-Meitner-Institut für Kernforschung Berlin GmbH, Nuclear Chemistry and Reactor Division

(Z. Naturforsch. **29 a**, 1742–1749 [1974]; received September 27, 1974)

The release of helium from neutron-irradiated Ag-9.6 at.-% Li-alloy is measured in the range between 510 and 784 °C. Analytical expressions are developed taking into account a recoil modified concentration profile in a surface layer. The isothermal kinetics can be described to some extent with two parameters, the effective diffusion coefficient p^2D and the absorption coefficient μ of helium in traps. From foil-experiments the untrapped fraction p of gas after irradiation is found to be $0.2 \leq p \leq 1$ for a helium concentration of $1.1 \cdot 10^{-5}$ at.-%. The activation energy of diffusion is found to be 1.7 eV, which indicates a vacancy mechanism. The absorption coefficient μ is of the order of some 10^{-4} [sec $^{-1}$] and nearly independent of temperature. It is discussed whether the diffusion to the traps or the capture process itself with a negative activation entropy is rate determining. The method seems to be applicable to incomplete degassing of other gas-metal-systems described in the literature.

Introduction

Helium from (n, α)-reactions in nuclear or proposed fusion reactor materials is of great importance because on the one hand helium tends to form bubbles, which cause high temperature embrittlement^{1,2}, or supports strongly the nucleation of voids on the other hand^{3,4}. Therefore, the kinetics of helium-bubble formation at higher temperatures is the subject of many investigations, especially using electron microscopy⁵⁻⁷. This method is, however, only valid for helium concentrations greater than about 10^{-4} at.-%, which is much higher than that in the nucleation stage of bubbles. Therefore the diffusion behaviour of helium was often studied using the more sensitive degassing experiments during linear temperature rise annealing⁸⁻¹⁰. However, there are only few isothermal helium release measurements. In Al incomplete degassing of helium was observed¹¹, while in Mg no permanent trapping of helium was found¹².

Recently Garside¹³ observed incomplete degassing of helium from silver after homogeneous He-ion-implantation. The data of these isothermal experiments were treated only in terms of diffusion. As a consequence decreasing diffusion coefficients with increasing annealing time resulted. However, permanent trapping may be described more realistically by a diffusion equation with an additional absorption term^{14,15}. In this way one may obtain numerical values for the diffusion and the absorption coefficients simultaneously from experiments. Results of further analytical calculations are compared in this paper with the isothermal release of helium from a silver-lithium alloy after neutron irradiation. During annealing of the samples only a small surface layer was degassed while the gas in the interior became permanently trapped. Therefore, onedimensional calculations could be applied. The initial depletion of gas in the surface resulting from escape by recoil during irradiation was taken into account.

Experimental

The silver alloy with 9.6 at.-% Li (7.42% Li-6) was prepared by Dr. E. Dürrwächter, Döduco KG, from 99.99% Ag and 99.8% Li. Samples of $(12 \times 7 \times 2)$ mm³ were annealed 20 minutes at 480 °C in high vacuum. The mean grain size then was 15 μ m. Samples were irradiated in the SSW-channel of the thermal reactor BER I to a thermal fluence of 3.6×10^{16} /cm². The temperature of irradiation was about 30 °C. As a result of the reaction Li-6(n, α) H-3 the samples contained 1.1×10^{-5} at.-% Helium and Tritium respectively. The gas was distributed uniformly except near the surface where loss due to recoil occurs. However, this inhomogeneous gas distribution was eliminated in foils (thickness $\geq 35 \mu$ m) which were closely pressed one on another and irradiated all together in a packet. Another advantage of using thin foils is the higher fraction of gas leaving the sample, which allows conclusions concerning the fraction p of untrapped gas in the beginning.

Reprint requests to Dr. H. Gaus, Hahn-Meitner-Institut für Kernforschung, Bereich C, D-1000 Berlin 39, Glienicke Str. 100.



Dieses Werk wurde im Jahr 2013 vom Verlag Zeitschrift für Naturforschung in Zusammenarbeit mit der Max-Planck-Gesellschaft zur Förderung der Wissenschaften e.V. digitalisiert und unter folgender Lizenz veröffentlicht: Creative Commons Namensnennung-Keine Bearbeitung 3.0 Deutschland Lizenz.

Zum 01.01.2015 ist eine Anpassung der Lizenzbedingungen (Entfall der Creative Commons Lizenzbedingung „Keine Bearbeitung“) beabsichtigt, um eine Nachnutzung auch im Rahmen zukünftiger wissenschaftlicher Nutzungsformen zu ermöglichen.

This work has been digitalized and published in 2013 by Verlag Zeitschrift für Naturforschung in cooperation with the Max Planck Society for the Advancement of Science under a Creative Commons Attribution-NoDerivs 3.0 Germany License.

On 01.01.2015 it is planned to change the License Conditions (the removal of the Creative Commons License condition “no derivative works”). This is to allow reuse in the area of future scientific usage.

The irradiated samples were isothermally annealed in a static high vacuum system connected with a MS-10 mass spectrometer. During a diffusion run an Ultek-Ti-getterpump kept the pressure always below 10^{-5} Torr. Thus continuous monitoring of helium from the very beginning of the experiment was possible. The effective sensitivity of the apparatus was about 10^{-10} cm³ NTP limited by a linear increase of the He background due to incoming of atmospheric He. Since this increase was constant with an accuracy of $\pm 10\%$ during the whole experiment it could be taken into account sufficiently. After every diffusion run the sample was melted in order to determine the total amount of helium. In the case of the foils weight loss by evaporation was determined before melting the sample. Since this loss was lower than $10^{-2}\%$ it was not taken into account.

Mathematical Treatment of the Kinetics

For a simple description of the gas release we use the diffusion equation with absorption term

$$\partial c / \partial t = D \Delta c - \mu c \quad (1)$$

$c = c(x, t)$ = concentration of the not trapped gas atoms [cm⁻³],

D = diffusion coefficient [cm²/sec],

μ = absorption coefficient [sec⁻¹].

We take D and μ as constant. In this equation neither an eventual partial emission of the absorbed gas nor any nonlinear effect (such as concentration dependence) is taken into account explicitly because there is no certain knowledge of the absorption process. For the present we consider the sample as infinite with a plane surface. We may calculate the resulting gas release and apply this result on a finite sample for a time during which the diffusion depth $2\sqrt{Dt}$ is small compared to the sample dimensions R .

$$2\sqrt{Dt} \ll R.$$

$$\text{If } 2\sqrt{D/\mu} \ll R \quad (1a)$$

is fulfilled, this time covers the whole time of gas release.

a) Nonuniform Initial Concentration with Absorption

We consider an initial concentration resulting from escape by recoil during irradiation¹⁶

$$\begin{aligned} c(x, 0) &= c_0[a + (1-a)x/r_0] \quad \text{for } 0 \leq x \leq r_0, \\ &= c_0 \quad \text{for } r_0 \leq x, \end{aligned} \quad (2)$$

x = distance from the surface [cm],

r_0 = recoil range [cm],

a = fractional number (e. g. 1/2).

In the mentioned way one gets for the fraction of the released gas

$$F(t) = \left[1 - \frac{1}{2} (1-a)r_0 \frac{S}{V} \right]^{-1} p \frac{S}{V} f(t). \quad (3)$$

Here S and V are the surface of the sample and the volume respectively. The factor $p \leq 1$ allows that at $t=0$ the fraction $(1-p)$ of the gas may be captured and does not participate in the diffusion. The function $f(t)$, dimension [cm], becomes (see appendix):

$$f(t) = \sqrt{\frac{D}{\mu}} \left\{ a \operatorname{erf}(\sqrt{\zeta}) + \frac{1-a}{2} \frac{1}{B} \cdot \int_0^{\zeta} e^{-\zeta'} \operatorname{erf}(B/\sqrt{\zeta'}) d\zeta' \right\} \quad (4)$$

with

$$\zeta = \mu t, \quad B = \frac{r_0}{2} \sqrt{\frac{\mu}{D}}, \quad \operatorname{erf} x = \frac{2}{\sqrt{\pi}} \int_0^x e^{-u^2} du. \quad (5)$$

By interchanging the order of integration in the second term one may bring $f(t)$ into the form

$$f(t) = \sqrt{\frac{D}{\mu}} \left\{ a \operatorname{erf}(\sqrt{\zeta}) + \frac{1-a}{2} \cdot \left[\frac{1}{B} (1 - e^{-\zeta}) + \frac{2}{\sqrt{\pi}} \int_{1/\sqrt{\zeta}}^{\infty} e^{-B^2 x^2} (e^{-\zeta} - e^{-1/x^2}) dx \right] \right\}. \quad (6)$$

For $t = \zeta = \infty$ the integration can be performed yielding

$$f(\infty) = \sqrt{\frac{D}{\mu}} \left\{ a + \frac{1-a}{2B} (1 - e^{-2B}) \right\}. \quad (7)$$

For $B \gtrsim 3$ the exponential term may be neglected and correspondingly one gets

$$f(t) = \left\{ a \operatorname{erf}(\sqrt{\zeta}) + \frac{1-a}{2B} [1 - e^{-\zeta} \operatorname{erf}(B/\sqrt{\zeta})] \right\} \times \sqrt{D/\mu} \quad (8)$$

for $B \gtrsim 3$.

When applying these equations we replace $\sqrt{D/\mu}$ by $r_0/2B$; cf. (5). Assuming at first $p=1$ we have the two parameters B and μ to adjust the calculated curves to the experimental ones, which is equivalent to the determination of D and μ . From (3) and (7)

one gets $F(\infty)$ as a function of B . Drawing this function one may also determine the value of B to a given experimental $F(\infty)$. Knowing B one gets the value of μ via D . The value of D essentially determines the behaviour of $F(t)$ for small times. As customary, one may draw $F^2(t)$ versus t . An evaluation of Eq. 4 yields

$$f^2(t) = \frac{4a^2}{\pi} D \left[t + \frac{1-a}{a} \frac{\sqrt{\pi D}}{r_0} \cdot t^{3/2} - \left(\frac{2\mu}{3} - \left(\frac{1-a}{2a r_0} \right)^2 \pi D \right) t^2 + \dots \right] \quad (9)$$

However, practically it is not possible to determine D from the first term in this equation for two reasons. Firstly, in our case the higher powers of t become important to soon. Regarding plots of $F^2(t)$ from computer calculations of (6) it turns out to be impossible to draw the tangent accurately at $t=0$. Instead, the plots show after a small time, a relatively long linear ascent, which is larger by a factor of about 1,5 than the theoretical value at $t=0$. In some cases this ascent can be described with the approximation (9), in other cases even higher terms become important. Thus strictly speaking one must describe also the initial ascent by a combination of D and μ compatible with the value of B given by $F(\infty)$. However, a variation of μ is of minor importance.

The second reason is the modification of the initial degassing by the finite time of temperature rise at the beginning. A comparison with the theoretical plot (for sudden temperature rise) is meaningful only some time after the temperature rise.

b) Nonuniform Initial Concentration without Absorption

In the above formulas of course one may pass also to the limit $\mu=0$; the result is

$$f(t) = a 2 \sqrt{\frac{D t}{\pi}} + \frac{1-a}{2} r_0 \cdot \left\{ \left(1 + \frac{\eta^2}{2} \right) \operatorname{erf} \left(\frac{1}{\eta} \right) - 1 + \frac{\eta}{\sqrt{\pi}} e^{-1/\eta^2} \right\} \quad (10)$$

wherein $\eta = (2/r_0) \sqrt{D t}$.

An equivalent formula was published earlier by Olander and Pigford¹⁷. For sufficient small times ($\eta \leq 0.5$) this may be replaced by

$$f(t) = 2 \sqrt{\frac{D t}{\pi}} \left[a + (1-a) \left\{ \frac{\sqrt{\pi}}{4} \eta - \eta^4 e^{-1/\eta^2} \right\} \right] \quad (11)$$

Equation (10) and (11) are not applied in the present paper.

c) The Initially Diffusing Fraction p

For a uniform initial concentration one gets from (3) and (4) with $r_0=0$

$$F(t) = p \frac{S}{V} \sqrt{\frac{D}{\mu}} \operatorname{erf} \sqrt{\mu t}. \quad (12)$$

In this case it is impossible to determine D and p separately. One may eliminate p by putting

$$D_p = p^2 D \quad (13)$$

and consider D_p as the measurable quantity.

In principle a nonuniform initial concentration yields more information in this respect. But as expected it turns out that within a certain range a

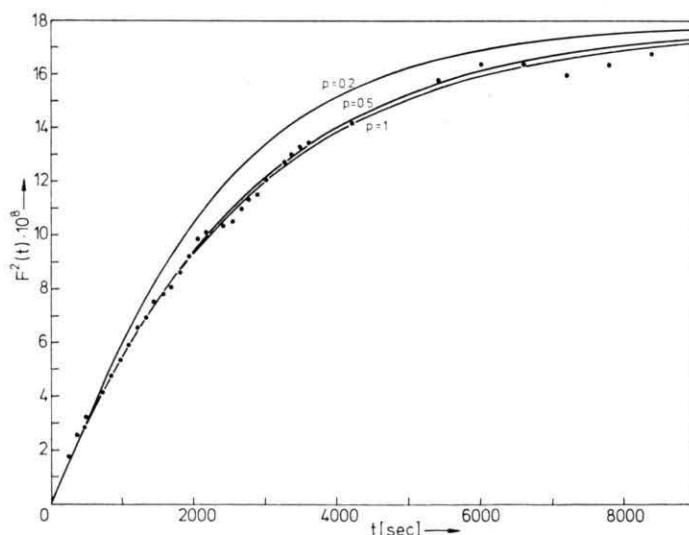


Fig. 1. Helium degassing (full points) in agreement with Eq. (3) and (4) for values of $p=1.0$, $D=9.15 \cdot 10^{-13} \text{ cm}^2 \text{ sec}^{-1}$, $\mu=3.34 \cdot 10^{-4} \text{ sec}^{-1}$ or $p=0.5$, $D=3.37 \cdot 10^{-12} \text{ cm}^2 \text{ sec}^{-1}$, $\mu=3.6 \cdot 10^{-4} \text{ sec}^{-1}$ respectively. The plot for $p=0.2$, $D=1.93 \cdot 10^{-11} \text{ cm}^2 \text{ sec}^{-1}$ and $\mu=4.43 \cdot 10^{-4} \text{ sec}^{-1}$ deviates from the measurement. Sample with recoil profile, $T=554^\circ \text{C}$.

variation of p in (3) can be compensated by a variation of D like the one given by (13) and a slight variation of μ . An example is shown in Figure 1. The curves are adjusted by changing B , μ , and p keeping fixed the $F(\infty)$ and the initial ascent. Agreement can be reached with values $p=1$ up to $p=0.5$. For an even smaller value a deviation results, in this case the curvature is enlarged. This effect of a diminution of p depends on the parameters, especially on the value of B . The change of the curve may go also into the opposite direction to that of Figure 1. It can be seen from Fig. 1, that also in case of a nonuniform initial concentration a safe determination of p is not possible.

Therefore we put $p=1$ throughout and consider the determined diffusion coefficients as $p^2 D$ values (13), which is exact for uniform initial concentration and a sufficient approximation for nonuniform initial concentration. This way there are only the two parameters D and μ to adjust the calculated curves.

Results

For simplicity of representation and ease of interpretation the experimental data were plotted as $F^2(t)$ versus time. This plot was compared with calculations according to (3) and (4) or to (12) in case of foils with uniform gas concentration. The theoretical curve was regarded as optimal if the constant ascent in the beginning and the part near $F(\infty)$ were optimized. The corresponding values of D and μ were obtained by trial and error. In case of samples with recoil profile this was done in the way described above after Equation (8). A problem sometimes arose from the fact that $F(\infty)$ was not reached although the measurements were carried out over several hours. In this case the curves were adjusted to the latest measured $F(t)$ -values.

a) Samples with Recoil Profile

Out of eight measurements two agree well with (3), (4). As an example Fig. 1 shows the kinetics at 554 °C. In the other experiments the median part of the experimental curve runs up to 15% below the theoretical curve, as can be seen from Figure 2. Table 1 shows the values of D and μ and an approximated D' , which results using only the first term in (9). As can be seen the absorption coefficient μ seems to be nearly independent of temperature.

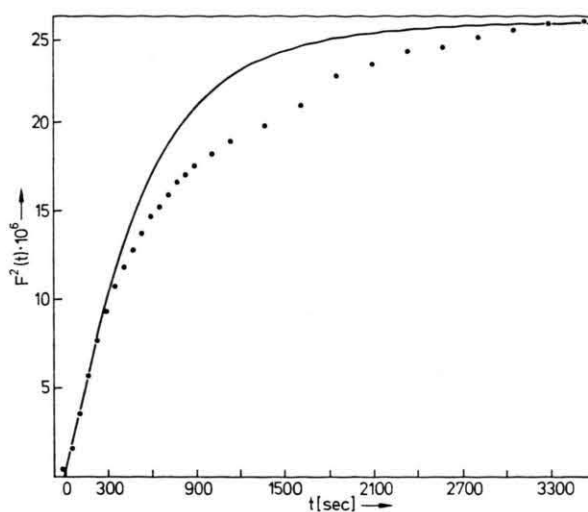


Fig. 2. Helium degassing (full points) deviating from Eq. (3) and (4). The closed line is a plot for $p=1$, $D=3.21 \cdot 10^{-10} \text{ cm}^2 \text{ sec}^{-1}$, $\mu=1.72 \cdot 10^{-3} \text{ sec}^{-1}$. Sample with recoil profile, $T=742^\circ \text{C}$.

Tab. 1. Coefficients of diffusion and absorption of helium in an Ag-9.6 At.% Li-alloy obtained from samples with recoil profile by applying Eq. (3), (4) with $p=1$. The value of S/V is 14.5 cm^{-1} .

Temperature [°C]	Diffusion coefficient [cm ² ·sec ⁻¹]		Absorption coefficient [sec ⁻¹]
	D	D'	μ
510	$2.85 \cdot 10^{-13}$	$3.16 \cdot 10^{-13}$	$1.23 \cdot 10^{-4}$
554	$9.15 \cdot 10^{-13}$	$8.75 \cdot 10^{-13}$	$3.34 \cdot 10^{-4}$
625	$1.03 \cdot 10^{-11}$	$1.27 \cdot 10^{-11}$	$3.08 \cdot 10^{-4}$
695	$1.0 \cdot 10^{-11}$	$1.55 \cdot 10^{-11}$	$2.63 \cdot 10^{-4}$
698	$3.82 \cdot 10^{-11}$	$6.48 \cdot 10^{-11}$	$3.45 \cdot 10^{-4}$
738	$7.52 \cdot 10^{-11}$	$1.33 \cdot 10^{-10}$	$2.29 \cdot 10^{-4}$
742	$3.21 \cdot 10^{-10}$	$4.96 \cdot 10^{-10}$	$1.72 \cdot 10^{-3}$
784	$1.51 \cdot 10^{-10}$	$3.0 \cdot 10^{-10}$	$4.48 \cdot 10^{-4}$

b) Foils without Recoil Profile

Out of eight measurements three, like the one in Fig. 3, agree well with Equation (12). In the other five experiments there is a deviation in the median part of the plot to lower F^2 -values similar to the kinetics of the thick samples. The resulting values of D and μ from the foil experiments together with the values of $F(\infty)$ are collected in Table 2. From the highest value of $F(\infty)$ one may estimate $0.2 \leq p \leq 1$.

As in case of the thick samples the absorption coefficient μ seems to be nearly independent of temperature. This statement means that $F(\infty) V/S$ increases with temperature like $D^{1/2}$ since according

Tab. 2. Coefficients of diffusion and absorption of helium in an Ag-9.6 At.% Li-alloy, obtained from foils with initially uniform concentration by applying Eq. (12) with $p=1$.

S/V [cm ⁻¹]	Tem- pera- ture [°C]	$F(\infty)$	Diffusion coefficient D [cm ² ·sec ⁻¹]	Absorption coefficient μ [sec ⁻¹]
55.5	543	$3.51 \cdot 10^{-3}$	$4.57 \cdot 10^{-12}$	$1.09 \cdot 10^{-3}$
229	543	$2.02 \cdot 10^{-2}$	$1.38 \cdot 10^{-11}$	$1.77 \cdot 10^{-3}$
77.3	600	$9.62 \cdot 10^{-3}$	$2.1 \cdot 10^{-11}$	$1.31 \cdot 10^{-3}$
224	600	$3.25 \cdot 10^{-2}$	$4.17 \cdot 10^{-11}$	$2.34 \cdot 10^{-3}$
225	600	$3.27 \cdot 10^{-2}$	$1.75 \cdot 10^{-11}$	$7.81 \cdot 10^{-4}$
122	700	$4.7 \cdot 10^{-2}$	$3.39 \cdot 10^{-10}$	$2.44 \cdot 10^{-3}$
226	700	$7.3 \cdot 10^{-2}$	$2.71 \cdot 10^{-10}$	$2.81 \cdot 10^{-3}$
575	700	$2.0 \cdot 10^{-1}$	$3.79 \cdot 10^{-10}$	$3.34 \cdot 10^{-3}$

to Eq. (12)

$$F(\infty) = p \frac{S}{V} \sqrt{\frac{D}{\mu}}$$

and μ is adjusted in all cases to fit the latest F -values as described above. Further, from this it can be excluded that only the grains adjacent to the surface contribute to degassing while the gas of the internal grains is absorbed completely by the grain boundaries, for in this case $F(\infty) V/S$ would be essentially independent of temperature.

c) Arrhenius Diagram

Figure 4 shows an Arrhenius-plot of the $p^2 D$ -values of both kinds of samples. In case of foils one gets $p^2 D = 0.127 \exp\{-1.67 \text{ eV}/kT\}$ [cm² sec⁻¹] and in case of thick samples $p^2 D = 0.0341 \exp\{-1.73 \text{ eV}/kT\}$ [cm² sec⁻¹]. There is a dif-

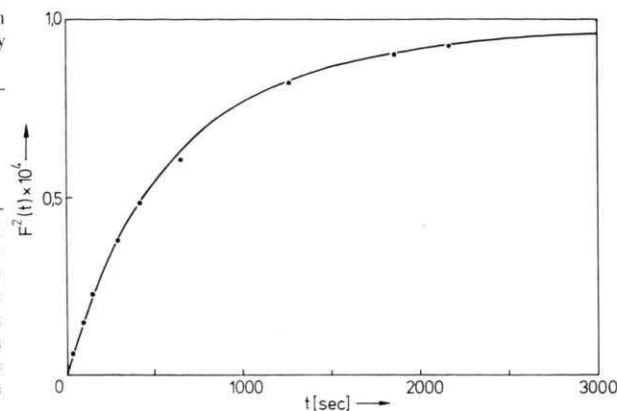


Fig. 3. Helium degassing (full points) in agreement with Equation (12). The closed line is a plot for $p^2 D = 2.11 \cdot 10^{-11} \text{ cm}^2 \text{ sec}^{-1}$, $\mu = 1.31 \cdot 10^{-3} \text{ sec}^{-1}$. Sample with initially uniform concentration, $T = 600^\circ \text{C}$.

ference in the frequency factors, while the activation energies can be regarded as equal. Also shown are the results in pure silver obtained by Garside¹³ as initial values of his time dependent D for He concentrations of $10^{-6} \text{ at.}\%$ and $10^{-4} \text{ at.}\%$ respectively. These initial values correspond to the application of Eq. (12) with $p=1$. In our case the concentration was $1.1 \times 10^{-5} \text{ at.}\%$. Taking into account the difference in concentration and material our results can be regarded as in agreement with those of Garside.

The S/V -values of the foils at a given temperature differ by factor up to 4. Inserting one and the same S/V -value of a single grain of the polycrystalline samples yields unreasonably much more different

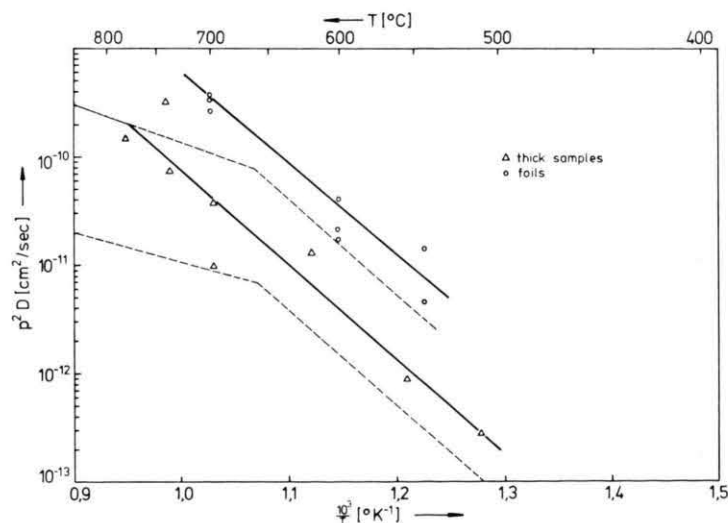


Fig. 4. Temperature dependence of the diffusion coefficient $p^2 D$ of helium in Ag 9.6 At.% Li. The broken lines are obtained for pure silver by Garside¹³ for He-concentrations of $10^{-6} \text{ At.}\%$ (upper curve) and $10^{-4} \text{ At.}\%$ (lower curve) respectively.

D -values for the same temperature than the values in Table 2. Thus, it is concluded that grain boundary diffusion is not remarkably faster than volume diffusion. The obtained D -values may correspond to an overlapping of both processes.

Figure 5 shows an Arrhenius-plot of the quotients (μ/D) . In contrast to Fig. 4 the difference between the foils and the thick samples disappears. The temperature dependence of (μ/D) can be described by $\exp \{1.35 \text{ eV}/kT\}$.

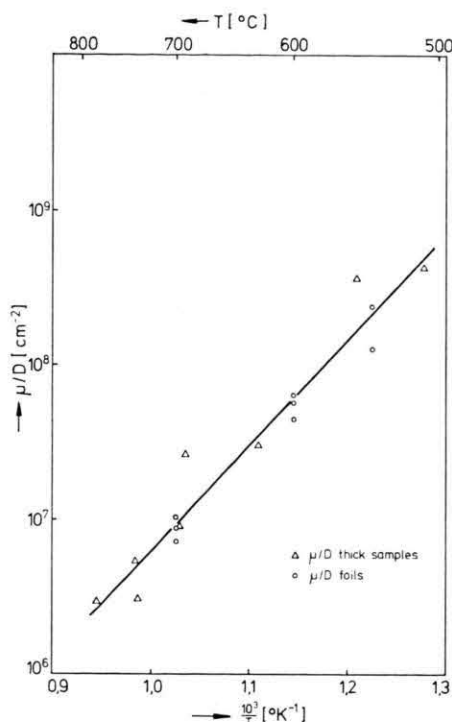


Fig. 5. Temperature dependence of the quotient (μ/D) with $p=1$.

Discussion

The measured activation energies of diffusion of He in the alloy indicate a process of diffusion supported by vacancies. For this process Wilson and Bauer¹⁸ calculated in the system Ag-He a value of 1.53 eV, while an interstitial mechanism results in 0.86 eV. Very recently Wilson and Bisson¹⁹ did more detailed calculations for He in copper and tungsten. The results favour an exchange mechanism of a vacancy-captured helium with a host atom. The authors find the rate-limiting step to be the jump of the helium out of the vacancy the activation

energy for which is 2.15 eV in copper. — Concerning the absorption coefficient μ an approach sometimes used and discussed especially by Waite^{20, 21} would be for the present case: Whenever a diffusing helium atom approaches an absorption center to a distance r within $r_1 \leq r \leq r_1 + \Delta r_1$ there is a definite probability $\lambda [\text{sec}^{-1}]$ of absorption. As usual one assumes

$$\lambda = \lambda_0 e^{-Q/kT} \quad (14)$$

with a frequency factor λ_0 and an activation enthalpy Q . The coefficient λ_0 contains the factor $\exp \{AS/k\}$, where AS is the activation entropy. In the usual rate theory $AS = S_a - S_0$ where S_a and S_0 denote the entropies of the saddlepoint and the equilibrium configuration respectively. Now, according to Waite²¹ for times when the diffusion depth is larger than r_1 , that is for

$$\sqrt{Dt}/r_1 \gg 1, \quad (15)$$

the absorption coefficient μ from Eq. (1) should be

$$\mu = 4 \pi r_1 D \frac{s}{s+1} C_B \quad (16)$$

where

$$s = \lambda r_1 \Delta r_1 / D \quad (17)$$

and C_B is the number of trapping centers per cm^3 .

If $s \gg 1$, in Eq. (16) s and hence λ drops out and the absorption is diffusion controlled

$$\mu = 4 \pi r_1 D C_B. \quad (18)$$

If on the contrary $s \ll 1$, there results

$$\mu = \lambda \cdot 4 \pi r_1^2 \Delta r_1 C_B. \quad (19)$$

The diffusion is rapid enough to maintain a random distribution in spite of the absorption. Equations (18) and (19) are immediately clear containing a characteristic length denoted $4 \pi r_1$ and reaction volume denoted $4 \pi r_1^2 \Delta r_1$.

From the fact that μ/D is equal for both cases, foils and thick samples (Fig. 5), one would conclude that (18) and $s \gg 1$ is realized. Then one has to assume a temperature dependence of C_B according to Figure 5:

$$\mu/D \cdot 4 \pi r_1 = C_B \approx C_B^0 \exp \{1.35 \text{ eV}/kT\}, \quad (20)$$

in the investigated temperature range. This could be attributed to an annealing process yielding a more complicated temperature dependence which may be approximated by (20) in the mentioned range. Such annealing could also continue during the isothermal measurement resulting in a decreasing

μ with time. This could well cause the deviation shown in Figure 2. In order to see the effect of a time decreasing μ in case of foils we performed calculations with $\mu = a + b/\sqrt{t}$ because this form is integrable, but with this form no quantitative statement concerning the deviation in the curves is possible.

If (19) is realized one may consider C_B as temperature independent and $Q = -0.35$ eV in Equation (14). In this case the differences in D and μ , comparing foils and thick samples, could be attributed to differences in the degassed layers of the samples yielding the same factor for D and μ corresponding to Figure 5. If grain boundary diffusion is rate determining and the absorption takes place on the grain boundaries a common factor seems possible.

From $s \ll 1$ it follows by (17) and (19) instead (20)

$$\mu/D \, 4\pi r_1 \ll C_B. \quad (21)$$

Now, with the largest value $4 \cdot 10^8 \text{ cm}^{-2}$ for μ/D and $r_1 \approx 2 \text{ \AA}$ (corresponding to a length of only one lattice parameter) one obtains for the left side of (21) about 10^{15} cm^{-3} . For a larger r_1 e.g. for the radius of a secondary defect, a smaller value results. Garside¹³ concluded from special experiments that the trapping of He in silver is due to an interaction of the heliums themselves yielding a homogeneous nucleation of bubbles. In our case the concentration of helium was $6.4 \cdot 10^{15} \text{ cm}^{-3}$. Taking this value for C_B and putting $r_1 \approx \Delta r_1 \approx 10^{-8} \text{ cm}$ one obtains from (19) for the foils

$$\lambda = 2 \cdot 10^6 \exp \{ -0.35 \text{ eV} / kT \} [\text{sec}^{-1}].$$

Assuming secondary defects as traps one would estimate a concentration some times smaller but r_1^2 about hundred times larger than for the single

heliums yielding an even smaller value for λ_0 . Such frequency factors λ_0 , some orders of magnitude smaller than kT/h , indicate a negative activation entropy, $S_a < S_0$. They are discussed in gas absorption theory^{22, 23} and were observed too for the emission of tritium from traps in an Ag-Li-alloy²⁴. The values indicate that the activated complex is a somewhat complicated configuration.

Garside's assumption is consistent with our results assuming $s \ll 1$, i.e. (19), but we cannot exclude another absorption process, e.g. the absorption by secondary defects. In view on this uncertainty we do not discuss the time behaviour of μ via C_B , if C_B is given by the heliums themselves. Without Garside's results we cannot decide whether (18) or (19) is valid²⁵.

Garside investigated concentrations of He in the range from $10^{-6} \text{ At.}\%$ to $10^{-2} \text{ At.}\%$. He obtained a diminution of his initial D with increasing concentration. This effect may be due however, to a decrease of p , as the measured quantity is $p^2 D$. It is rather likely that at higher concentrations a larger fraction of helium is captured already during irradiation, compare for example reference⁶.

Appendix

In order to calculate the gas release for the non-uniform initial concentration (2) we first transform Eq. (1) by putting

$$c(x, t) = g(x, t) e^{-\mu t}$$

to obtain

$$\partial g / \partial t = D \Delta g.$$

We have

$$g(x, 0) = c(x, 0)$$

and the boundary condition

$$g(0, t) = c(0, t) = 0.$$

We use the well known solution

$$g(x, t) = \frac{1}{2\sqrt{\pi Dt}} \int_0^\infty g(\xi, 0) \left(\exp \left\{ -\frac{(x-\xi)^2}{4Dt} \right\} - \exp \left\{ -\frac{(x+\xi)^2}{4Dt} \right\} \right) d\xi.$$

Interting for $g(\xi, 0)$ Eq. (2) with $c_0 = 1$, differentiating with respect to x and then putting $x = 0$, we obtain

$$\frac{d}{dx} g(x, t) \Big|_{x=0} = \frac{1}{2\sqrt{\pi Dt}} \left\{ \int_0^\infty \frac{\xi}{Dt} \exp \left\{ -\frac{\xi^2}{4Dt} \right\} d\xi - (1-a) \int_0^{r_0} \left(1 - \frac{\xi}{r_0} \right) \frac{\xi}{Dt} \exp \left\{ -\frac{\xi^2}{4Dt} \right\} d\xi \right\}.$$

In the first term the integration may be performed, in the second term it may be simplified by partial integration. Multiplying by $\exp -\mu t$ we get

$$\frac{d}{dx} c(x, t) \Big|_{x=0} = \frac{e^{-\mu t}}{\sqrt{\pi D t}} \left\{ a + \frac{1-a}{r_0} \int_0^{r_0} \exp \left\{ -\xi^2/4 D t \right\} d\xi \right\}.$$

Multiplying this expression by D and integrating over t we obtain directly Equation (4).

-
- ¹ A. C. Roberts and D. R. Harris, *Nature London* **200**, 200 [1963].
- ² I. O. Smith, B. Russel, *J. Nucl. Mat.* **38**, 1 [1971].
- ³ R. S. Nelson and D. J. Mazey, *Proc. Symp. on Radiation Damage in Reactor Materials*, Wien 2.-6. Juni 1969, p. 157.
- ⁴ R. Bullough and R. C. Perrin, *British Nuclear Energy Society, European Conference, Proceedings*, p. 79 [1971].
- ⁵ V. Levy, J. Antolin, J. Espinasse, and Y. Adda, *CEN Saclay, Rapport CEA R 2529* [1964].
- ⁶ O. Smith and B. Russell, *J. Nucl. Mat.* **35**, 137 [1970].
- ⁷ R. D. Brown, P. Rao, and P. S. Ho, *Radiation Effects* **18**, 149 [1973].
- ⁸ E. V. Kornelsen, *Canadian J. Physics*, **48**, 2812 [1970].
- ⁹ E. V. Kornelsen, *Radiation Effects* **13**, 227 [1972].
- ¹⁰ D. S. Whitmell and R. S. Nelson, *Radiation Effects* **14**, 249 [1972].
- ¹¹ H. R. Glyde and K. I. Mayne, *Phil. Mag.* **12**, 997 [1965].
- ¹² H. R. Glyde and K. I. Mayne, *Phil. Mag.* **12**, 919 [1965].
- ¹³ D. Garside, Ph. D. Thesis, University of Sussex, 1971.
- ¹⁴ H. Gaus, *Z. Naturforsch.* **200 a**, 1298 [1965].
- ¹⁵ L. c. ¹⁴, esp. Equation (2.4).
- ¹⁶ S. Flügge and K. E. Zimen, *Z. Phys. Chem.* **42**, 179 [1939].
- ¹⁷ D. R. Olander and T. H. Pigford, *Trans. American Nucl. Soc.* **6**, 130 [1963].
- ¹⁸ W. Bauer and D. W. Wilson, *Proc. USAEC International Conf. Albany*, June 9-11, 1971.
- ¹⁹ D. W. Wilson and C. L. Bisson, *Radiation Effects* **19**, 53 [1973].
- ²⁰ Th. R. Waite, *Phys. Rev.* **107**, 463 [1957].
- ²¹ Th. R. Waite, *J. Chem. Physics* **32**, 21 [1960].
- ²² D. A. Degras, *Suppl. Nuovo Cimento V*, 420 [1967].
- ²³ I. Lapujoulade, *Suppl. Nuovo Cimento V*, 433 [1967].
- ²⁴ H. Migge, *Phys. Stat. Sol.* **35**, 673 [1969].
- ²⁵ A diffusion controlled trapping of rare gases in ionic crystals is discussed in F. W. Felix, K. Meier, and M. Müller, *Z. Naturforsch.* **29 a**, 1299 [1974].